Chalcogenide Letters Vol. 11, No. 8, August 2014, p. 365 - 372

STRUCTURAL CHARACTERIZATION OF $Te_9Se_{72}Ge_{19-x}Sb_x$ ($8 \leq x \leq 12$) GLASS USING FAR-INFRARED SPECTRA

A. V. NIDHI[a*], V. MODGIL[b], V. S. RANGRA[b]
[a]*Department of Physics, Centre of Excellence, Government Degree College Sanjauli, Shimla, India*
[2]*Department of Physics, Himachal Pradesh University, Summerhill Shimla, India*

The chalcogenide alloy $Te_9Se_{72}Ge_{19-x}Sb_x$ *(8≤x≤12)* is investigated for its structure and glassy nature. The compositional variation of experimental and theoretical calculated value of glass transition temperature (T_g) has been studied and is supported by the theoretically calculated mean bond energy and cohesive energy. The bonding arrangement in the glass has been studied using far-infrared transmission spectroscopy. The results are interpreted using the chemical bond approach (CBA) and valence field force (VFF) model. All possible heteropolar bonds are observed in the material. A correlation between T_g and far IR results has also been predicted.

(Received May 23, 2014; Accepted August 1, 2014)

Keywords: Far infrared spectra; Glass transition temperature; Chalcogenide glass; Mean Bond energy

1. Introduction

The recent progress in the material science is influencing and inviting to explore or renovate the present research of chalcogenide glass to fulfil the requirement of advanced technology like phase change memory devices, fibre technology, inorganic photoresist, thermal imaging, bio sensing and pollutant detection [1-6]. The chalcogenide glasses are non oxide amorphous semiconductors having high transmission in the IR region [7] and exhibit some photoinduced phenomenon when exposed to the light having energy comparable to the band gap[8].The applications of chalcogenide glasses in the IR optics are mainly restricted by vibrational absorption bands of impurities introduced during the glass synthesis [9]. Different chalcogen based glasses have different transparency range, for example transparency region is located within spectral range 0.5μm–7μm for sulphur based, 0.8μm – 12μm for selenium based and 1.2μm – 16μm for tellurium based glasses[10]. So the Te-based glass fibres can be most useful in accurate detection of CO_2, which is being regarded as most polluted gas in earth atmosphere involving its two vibrational absorption bands at 4.3μm and 15μm [11].

There are several studies on Ge-Se-Sb glasses reported in the literature regarding their physical [12], electrical [13] optical [14] and thermal study [15] and chemical effects are also examined. Se-Ge-Sb glasses is one of the family that fulfils the requirements for fabrication of optical fibres such as large band gap, low dispersion, long wavelength multi phonon edge resulting in good thermal, mechanical, and chemical properties [16]. The material structure also has compositional dependence which also depends upon the mean coordination number variation. In order to explain the bonding arrangements in structural units of the material, 8N rule and chemical bond approach play their crucial role. S, Se and Te exhibit the two fold coordination number and require two neighbours to satisfy their valance requirement. The glasses formed from pure Se may consist of structural units such as Se_8 member ring and long helical chains held together by weak Van der Waals forces. The short comings associated with the pure Se glasses such as aging effect

*Corresponding author: avnidhi1@gmail.com

and thermal instability is eliminated with the addition of Ge which enhances material strength by increasing the crosslinking in the glassy network. The elements such as Sb causes the structural disorder which lead to tune the optical and thermal properties [17, 18] of material.

For the structural investigation of the material Raman or the FTIR techniques are most commonly used. Both these techniques are complementary to each other and any of these techniques can be used for structural investigation. In order to understand the properties of the glassy material it is necessary to analyze the structure and bonding arrangement of the material. Far infrared study has been reported therefore, in which all possible heteropolar bonds have been observed.

2. Experimental details:

2.1 Sample preparation and characterisation:

Bulk samples of $Te_9Se_{72}Ge_{19-x}Sb_x$ (x=8, 9, 10, 11, 12) chalcogenide glass has been prepared by conventional melt quenching technique. High purity materials in powder form (Se and Te (Alpha Aesar) and Ge and Te (Acros Organics)) are weighed according to their atomic weight percentage and sealed in evacuated quartz ampoules at a pressure of 5 x 10^{-5} milli bar. The sealed ampoules are kept inside a furnace, where the temperature is increased up to 1273 ^{o}K at a heating rate of 3–4 ^{o}K per min. These ampoules are frequently rocked for 15 h at highest temperature to make the melt homogeneous. The quenching is done in ice cold water. The material is extracted by breaking the ampoules and is grinded to powder using mortar and pestle. The nature of the different samples is investigated by Panalytical X'Pert-Pro diffractometer (PW 3050/60) by using Cu target source (λ = 1.5483 Å). Amorphous nature of the material is confirmed through XRD as there is the complete absence of sharp peaks in the diffractograms as shown in Fig. 1.

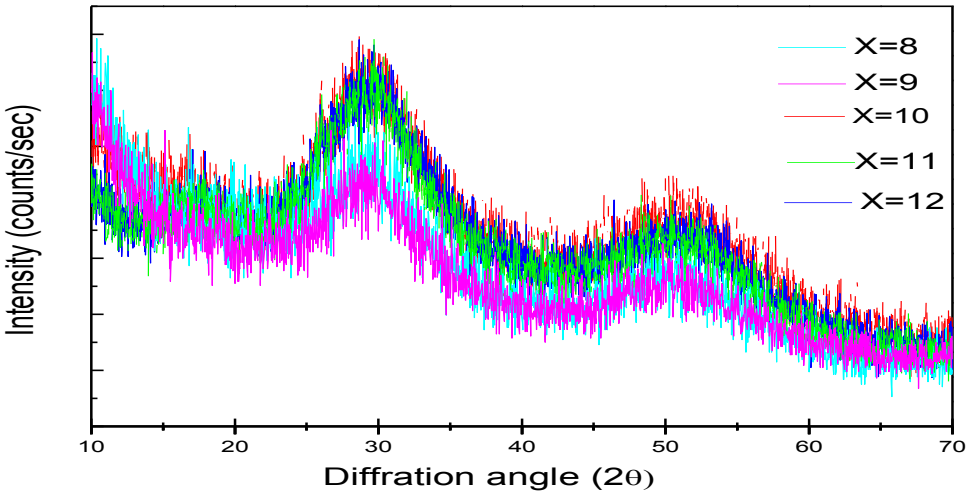

Fig.1. X- Ray diffractograms of the chalcogenide compositions $Te_9Se_{72}Ge_{19-x}Sb_x$ (8≤x≤12)

The far IR absorption spectra of different glassy alloys are obtained in spectral range (30–500) cm^{-1} at room temperature using (Perkin Elmer-Spectrum RX-IFTIR) FTIR Spectrometer with a resolution of 2 cm^{-1}. All the measurements are carried out using polythene pallet (13 mm diameter) method. The pellets are prepared by mixing 4 mg sample in powder form with 200 mg of spectroscopic grade polythene and then mixture is pressed using hydraulic press (~10 ton). To take account of polythene absorption, the spectrum of polythene was used as reference spectrum and finally the spectrum of the absorbed frequencies of the sample is obtained.

Glassy nature of the amorphous samples is investigated by taking approximately 15 mg quantity of each powdered samples using differential scanning calorimetery by DSC instrument

(Mettler Toledo DSC-1 of excellence series on high sensitivity sensor HSS-8). The samples are scanned at a constant heating rate of 10°K per minute to find out the glass transition temperature and peak crystallization temperature.

3. Results and discussion

3.1 Theoretical calculations of bond energy and relative bond formation:

There are the different types of bonds formed in the material. It becomes essential to analyze the structure of the material as different bonds have different energies and probabilities of formation. The bond energies of the possible bond formed in the composition $Te_9Se_{72}Ge_{19-x}Sb_x$ (x=8, 9, 10, 11, 12) is calculated using the Pauling Relation [19]

$$E_{A-B} = (E_{A-A}E_{B-B})^{1/2} + 30(\chi_A - \chi_B)^2 \quad (1)$$

Here χ_A and χ_B are the electronegativity of the atoms A and B and E_{A-A} and E_{B-B} are the bond energies of homopolar bonds respectively. The bond energy of the heteropolar bonds is calculated using the values tabulated in Table1 for homopolar bonds Ge-Ge, Se-Se, Sb-Sb and Te-Te respectively [20] and the electronegativity value 2.55, 2.10, 2.01 and 2.05 for Se,Te, Ge and Sb respectively [20]. The relative probabilities of bond formation have been calculated using the probability distribution function ($e^{-\frac{E}{k_bT}}$) at room temperature (300°K) and maximum heating temperature (1273°K). Where k_b is the Boltzmann constant and E is the bond energy. The values of some basic physical parameters used for structural analysis such as bond energy, reduced mass, force constant and probabilities of different possible bonds have been reported in Table 1.

Table 1 Values of bond energy, reduced mass (μ), force constant (K_{AB}), relative bond probability at 300°K and 1273°K in $Te_9Se_{72}Ge_{19-x}Sb_x$ (x=8, 9, 10, 11, 12) glassy system

Possible bonds	Bond energy (Kcal/mol)	Reduced mass (μ) x 10^{-26}(Kg)	Force constant (K_{AB}) x 10^5 dyne cm^{-1}	Relative bond probability	
				300°K	1273°K
Se-Ge	49.42	6.28	1.86	1	1
Se-Te	44.18	8.10	1.75	$1.52x10^{-4}$	$1.20x10^{-1}$
Se-Se	44.00	6.56	1.91	$1.12x10^{-4}$	$1.11x10^{-1}$
Se-Sb	43.95	7.95	1.54	$1.03x10^{-4}$	$1.10x10^{-1}$
Ge-Ge	37.60	6.03	1.29	$2.42x10^{-9}$	$8.64x10^{-3}$
Ge-Te	35.46	7.69	1.28	$6.68x10^{-11}$	$3.70x10^{-3}$
Ge-Sb	33.75	7.55	1.06	$3.79x10^{-12}$	$1.88x10^{-3}$
Te-Te	33.00	10.60	1.25	$1.08x10^{-12}$	$1.40x10^{-3}$
Sb-Te	31.64	10.34	1.05	$1.10x10^{-13}$	$8.17x10^{-4}$
Sb-Sb	30.20	10.11	0.87	$9.79x10^{-15}$	$6.42x10^{-4}$

3.2 Thermal analysis:

Differential scanning calorimetry has been carried out to obtain the thermograms of $Te_9Se_{72}Ge_{19-x}Sb_x$ (x=8, 9, 10, 11, 12) chalcogenide glass at heating rate of 10°K per minute and shown in the Fig. 2.

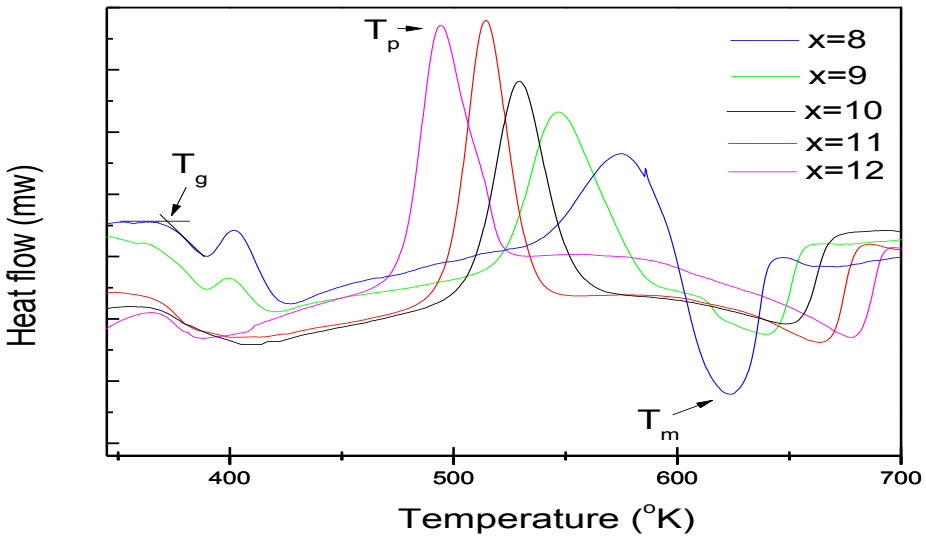

Fig. 2. DSC thermograms of $Te_9Se_{72}Ge_{19-x}Sb_x$ ($8 \le x \le 12$) at heating rate 10°K/minute

Experimentally measured Tg, Tp, theoretical calculated glass transition temperature by Lankhorst Model, mean bond energy and heat of atomization are listed in Table 2. There is a good agreement between the experimental value and theoretical calculated value of the glass transition temperature as both are approximately same and decreases with the rising antimony content as is being reported in our previous work on theoretical calculated parameters [20]. As the covalent radii of Sb (1.38Å) and Te (1.35 Å) are greater than the Ge (1.22 Å) and Se (1.16 Å), their addition introduces strain to the network and leads to a considerable weakening of the Se-Ge network structure. This results in the decrease of both the mean bond energy and glass transition temperature with increasing Sb content. The comparatively low bond energies of Sb-Se, Te-Se bonds than Ge-Se bond results in decrease in the mean bond energy and cohesive energy. Therefore the glass transition temperature also falls with rise in the Sb content.

Table 2. The glass transition temperature, peak crystallization temperature and theoretical calculated values of mean bond energy, heat of atomization and glass transition temperature (Lankhorst) of $Te_9Se_{72}Ge_{19-x}Sb_x$ (x=8,9,10,11,12).

Composition	Glass transition temperature T_g (°K)	Peak crystallization temperature T_p (°K)	Mean bond energy <E> Kcal/mol	Heat of atomization H_s Kcal/mol)	Lankhorst T_g (°K)
$Te_9Se_{72}Ge_{11}Sb_8$	371.02	574.47	51.35	58.18	357.98
$Te_9Se_{72}Ge_{10}Sb_9$	365.10	545.98	50.95	57.91	354.03
$Te_9Se_{72}Ge_9Sb_{10}$	367.18	529.38	50.54	57.63	350.07
$Te_9Se_{72}Ge_8Sb_{11}$	364.43	514.15	50.12	57.36	346.12
$Te_9Se_{72}Ge_7Sb_{12}$	362.06	493.75	49.72	57.08	342.16

3.3 Infrared spectroscopy

3.3.1 Qualitative studies

As there is no direct probe to study the structure of the amorphous material, far-infrared transmission spectroscopy is the best technique to find out the valuable information about the

structural arrangements of the glassy materials. Far IR transmission spectroscopy of the Te-Se-Ge-Sb glassy alloy has been carried out in (30-500) cm^{-1} range. In interpreting the results of FTIR spectra, the valence force field (VFF) model's[21] assumptions are taken as (i) there is a strong restoring force between the two valence bonds when the bond length or the angle between two bonds is changed. (ii) The position of the intrinsic IR features is mainly influenced by the stretching force constants of the corresponding chemical bonds. The wave number of the vibration modes of different bonds of material in the IR spectra is determined in terms of the reduced mass of the atoms and the inter-atomic force within the groups of atoms comprising glass network and is given by the relation

$$\nu = \frac{1}{2\pi c}\left(\frac{K_{AB}}{\mu}\right)^{1/2} \tag{2}$$

here K_{AB} is the bond stretching force constant of the bond between A and B and μ is the reduced mass of the molecule which is given by the following relation

$$\mu = \frac{M_1 M_2}{(M_1 + M_2)} \tag{3}$$

M_1 and M_2 are the atomic masses of the two atoms A and B respectively. In order to calculate the force constant K_{AB} between atoms A and B, the following authors have given the relations. First relation suggested by Gordy [22] which holds accurately for a large number of diatomic and simple polyatomic molecules in their ground state is given as

$$K_{AB} = aN\left(\frac{\chi_A \chi_B}{d^2}\right)^{3/4} + b \tag{4}$$

here a and b are constants which depend on the type of structural unit and d is the bond length. The bond order, N in the above equation can be found by using the expression

$$N = \frac{d + 2r_1 - 3r_2}{2d + r_1 - 3r_2} \tag{5}$$

here r_1 and r_2 are the covalent radii for the single bond and double bond respectively. Secondly, according to the relation given by Somayajulu [23], force constant can be calculated by the following relation

$$K_{AB} = (K_{AA}K_{BB})^{1/2} + (\chi_A - \chi_B)^2 \tag{6}$$

here K_{AA} and K_{BB} are the force constants for homopolar bonds A-A and B-B respectively and χ_A and χ_B are the electronegativity values of elements A and B respectively. The force constant values for homopolar (Se-Se, Ge-Ge, Sb-Sb and Te-Te) bonds and calculated value of possible heteropolar bonds in the material along with the respective values of K_{AB} and μ are listed in the Table 1.

3.3.2 Quantitative justification of some absorption bands

In order to explain the structural and physical properties of the chalcogenide glassy system many approaches have been proposed and one of them is the chemical bond approach (Bicerno and Ovshinsky) [24]. According to this approach combination in the atoms of different type take place more easily rather than in the atoms of same type. These bonds are formed in the sequence of decreasing bond energy until the available valence of atoms is saturated. The glass structure is assumed to be composed of cross linked structural units of heteronuclear bonds. IR spectra of the amorphous state can be compared to its counterpart in crystalline state to find the valuable information about the atomic configuration of the glasses.

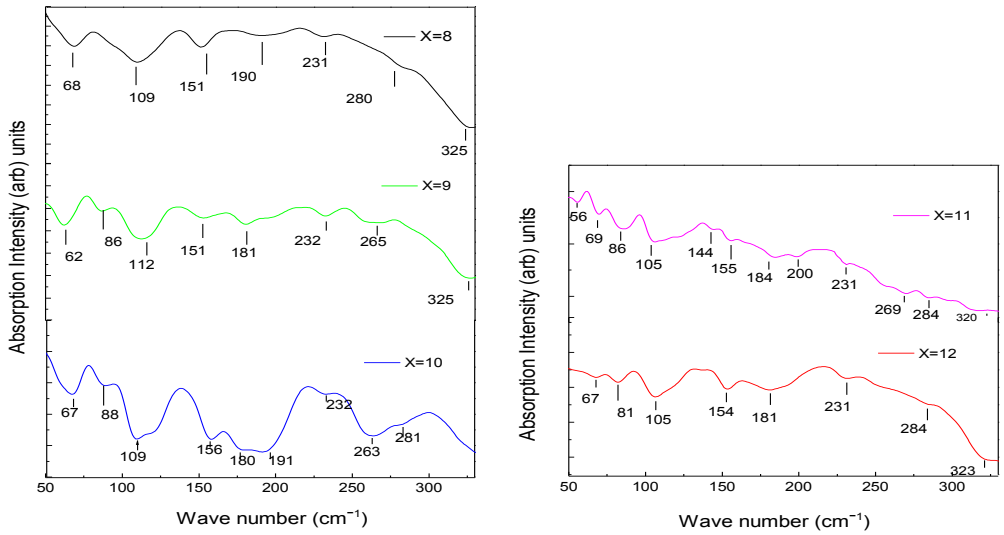

Fig. 3. Far IR spectra of of $Te_9Se_{72}Ge_{19-x}Sb_x$ ($8 \leq x \leq 12$)

Table 3 FTIR spectrum absorption peak assignments to various possible bonds in $Te_9Se_{72}Ge_{19-x}Sb_x$ (x=8, 9, 10, 11, 12) glassy system.

S. No.	x=8	x=9	x=10	x=11	x=12	Assignments
1	68	62,86	67,88	56,69,86	67,81	Se_8 (Rings)
2	109	112	109	105	105	Trigonal Se (A_2)mode
3	151	151	156	144, 155	154	$GeSe_2$ mode
4	-	181	180	184	181	$GeSe_2$ (Raman mode)
5	190	-	191	-	-	Sb-Se (bending mode)
6	-	-	-	200	-	Se-Te bond
7	231	232	232	231	231	$SbSe_3$ (stretching mode)
8	-	265	263	269	-	$GeSe_4$ (ν_3) mode
9	280	-	281	284	284	$Ge(Se_{1/2})_4$ structural units
10	325	325	-	320	323	Ge-Te bond

The far-infrared spectra of $Te_9Se_{72}Ge_{19-x}Sb_x$ where x=8, 9, 10, 11 and12 glassy composition are shown in Fig. 3 and respective wave numbers of different bonds are tabulated in Table 3. The absorption band 56 cm^{-1} - 90 cm^{-1} has been observed in all the samples confirming polymeric nature of the glass. The absorption peaks at 56 cm^{-1} and 62 cm^{-1} have been observed for the samples x=11 and x=9 respectively. The peak around 68 cm^{-1} is reported for the glassy composition at x=8, 10, 11 and 12. This observed band is due to the Se_8 (rings) in the material [25]. It is also observed that their intensity decreases with the composition, confirming that other defects increases and reduces the rings. These peaks diminish for x=11and 12. The absorption peak around 86 cm^{-1} is also appearing in the samples at x=9, 10, 11and 12. The similar observation has also been reported by Ohsaka [26] at 94 $cm^{-1}$for rings structure. The absorption peaks at 105 cm^{-1} for samples x=11and 12 , 109 cm^{-1} for x=8 and 10 and 112 cm^{-1} for x=9 are assigned to infrared active mode (A_2) of trigonal Se. Ohsaka [26] has also reported similar infrared active fundamental mode in the spectra of Se containing Te at 102 $cm^{-1}$for trigonal Se. $GeSe_2$ mode[25,27] has been observed at wave number 144 cm^{-1} in composition at x=11 and at 151 cm^{-1} for x=8, 9. The peak with lower intensity at around 155 cm^{-1} for samples x=10, 11, 12 has been observed as there is gradual decrease in the Ge concentration in the material. The peaks around 181 cm^{-1} are due to the $GeSe_2$ (Raman mode) observed in all the samples except x=8 [16]. The peak intensity around 151 $cm^{-1}$and 181 cm^{-1} diminishes at x=11and 12 which may be because of the decrease in Ge content as its atomic percentage varies from 11 to 7 in the matrix. The

absorption peak around 190 cm^{-1} has been found at x=8, 10 and assigned to Sb-Se bending mode. The absorption peak at 231 cm^{-1} is observed in the all samples and has been assigned to $SbSe_3$ stretching mode. A. B. Adam [28] has reported the band located between 190-210 cm^{-1} for Sb-Se bending mode and the band corresponding to 210-239 cm^{-1} with a shoulder at 220 cm^{-1} for $SbSe_3$ stretching mode. Sharma et al. [29] also assigned the band around 177-210 cm^{-1} to Se-Sb bond in Sb-Ge-Se glass. For the sample at x=11, the absorption peak at 200 cm^{-1} is assigned to Se-Te bond. Ohsaka[26] has reported the vibration of Se-Te bond at 205 cm^{-1}. The peaks observed at 265 cm^{-1}, 263 $cm^{-1}$and 269 cm^{-1} in samples at x=9,10 and11 respectively are assigned to $GeSe_4$ tetrahedral (ν_3) mode [16]. It has been found that absorption corresponding to this bond considerably diminishes after x=10. The absorption peak around 281 cm^{-1} observed in all the samples except x=9 is due to vibrations of nearly isolated F_2 mode of $Ge(Se_{1/2})_4$ tetrahedra which are connected with Se chains outside the clusters [30]. P Sharma et al. [27] has also reported a peak at 280 cm^{-1} for F_2 mode of $Ge(Se_{1/2})_4$ tetrahedra in $Ge_{10}Se_{90-x}Te_x$ semiconducting glassy alloy. S.A. Fayek [31] assigned the peak around 284 $cm^{-1}$to $Ge(Se_{1/2})_4$ structural units. The peaks at 325 cm^{-1} are observed for x=8, 9 and 320 cm^{-1},323 cm^{-1} at x=11, 12 respectively are assigned to the vibration of Ge-Te bond [32]. So it is being observed after the analysis of the far IR spectra that all possible heteropolar bonds are observed which is in accordance with the CBA and have compositional variation.

4. Conclusion

The material formed is amorphous and glassy in nature. The material possesses the high value of glass transition temperature (T_g) which falls with increase in the Sb concentration in the glassy matrix. This fall is because of the monotonic decrease in the cohesive energy and mean bond energy of the material as the stronger Ge-Se bonds are replaced by weaker Sb-Se bonds. Moreover the strain effect of Sb and Te is also responsible for structural weakening. The reported far-infrared results also confirm that Ge-Se bonds decrease and Sb-Se bonds increase as there an increase has been observed in absorption peak intensity of corresponding peak of Sb-Se with increasing Sb content. Obtained far IR results also support the behaviour of T_g in the glassy matrix.

References

[1] A.V. Kolobov, P. Fons, J. Tominaga, T. Uruga, J. Non-Cryst. Solids **352**, 1612 (2006).
[2] J. S Sanghera, L.B Shaw, I. D Aggarwal, Comptes Rendus Chimie **5**, 873 (2002).
[3] M. Mitkova, Thin Solid Films, **182**, 247 (1989).
[4] R. Hilton, Proc. SPIE **5786**, 258–261 (2005).
[5] A. A. Wilhelm; C. Boussard-Pledel, P. Lucas; M. R. Riley; B. Bureau; J. Lucas, Proc. SPIE **6433**, 1 (2007).
[6] K. Michel, B. Bureau, C. Boussard-Plédel, T. Jouan , J. L. Adam, K. Staubmann, T. Baumann, Sensors and Actuators , B **101**, 252 (2004).
[7] P. Sharma, S.C. Katyal, J. Non-Cryst. Solids **354**, 3836 (2008).
[8] K. Tanaka, A. Saitoh, N. Terakado, J. Mater Sci: Mater Electron, **20**, 38 (2009).
[9] A. B. Seddon, J. Non-Cryst. Solids. **184**, 44 (1995).
[10] V. Pamukchieva, K. Todorova, O. C. Mocioiu, M. Zaharescu, A. Szekeres, M. Gartner, J. Phys. Conf. Ser. **356**, 012047 (2012).
[11] G. Wang, Q. Nie, X. Wang, X. Shen, F. Chen,T. Xu, S. Dai, X. Zhang, J. Appl. Phys. **110**, 043536 (2011).
[12] P. Sharma, V. S. Rangra, S.C. Katyal, P. Sharma, Optoelectron. Adv. Mater. -Rapid Commun. **1**, 363 (2007).
[13] M. A. Afifi, H. H. Labib, M. H. El-Fazary, M. Fadel, Applied Physics A Solids and Surface, **55**, 167 (1992).

[14] F. A. Wahab, N. N. Ali karar, H. A. El Shaikh, R. M. Salem, Physica B Condensed Matter **422**, 40 (2013).
[15] E. R. Shaaban, I. B. I. Tomsah, J Therm Anal. Calorim, **105**, 191 (2011).
[16] D. R. Goyal, A.S. Maan, J. Non-Cryst. Solids **183**, 182 (1995).
[17] P. Sharma, V.S. Rangra, P. Sharma, S.C. Katyal, J. Alloys Compd. **480**, 934(2009).
[18] S. M. EI-Sayed, Semicond. Sci. Technol. **18**, 337 (2003).
[19] L. Pauling, The Nature of the Chemical Bond, Cornell University Press, New York, 1960.
[20] A. V. Nidhi, Vivek Modgil, V. S. Rangra, New Journal of Glass and Ceramics **3**, 91 (2013).
[21] I. Quiroga, C. Corredor, F. Bellido, J. Valázquez, P. Villares, R.J. Garay, J. Non-Cryst. Solids **196**, 183 (1996).
[22] W. Gordy, J. Chem. Phys. **14**, 305 (1946).
[23] G. R. Somayajulu, J. Chem. Phys. **28**, 814 (1958).
[24] J. Bicerano, S. R. Ovshinsky, J. Non-Cryst. Solids **75**, 169 (1985).
[25] G.J. Ball, J.M. Chamberlain, J. Non- Cryst. Solids **29**, 239 (1978).
[26] T. Ohsaka, J. Non-Cryst. Solids **22**, 359 (1976).
[27] P. Sharma, S. C. Katyal, J. Non-Cryst. Solids **354**, 3836 (2008).
[28] A. B. Adam, Journal of King Saud University (Science), **21**, 93 (2009).
[29] A. K. Sharma, K. L. Bhatia, V. K. Bhatnagar, S. K. Malik, J. Non-Cryst. Solids. **108**, 309 (1989).
[30] T. Fukunaga, Y. Tanaka, K. Murase, Solid State Commun. **42**, 513 (1982).
[31] S. A. Fayek, Infrared Physics & Technology **46**, 193-198 (2005).
[32] K. Nakamoto, Infrared and Raman spectra of inorganic and coordination compounds, PartA: John Wiley & Sons, Inc, fifth edition, New York, 1997.